

Stem Cell Reports, Volume 9

Supplemental Information

**Human Pluripotent Stem Cell-Derived Cardiac Tissue-like Constructs
for Repairing the Infarcted Myocardium**

Junjun Li, Itsunari Minami, Motoko Shiozaki, Leqian Yu, Shin Yajima, Shigeru Miyagawa, Yuji Shiba, Nobuhiro Morone, Satsuki Fukushima, Momoko Yoshioka, Sisi Li, Jing Qiao, Xin Li, Lin Wang, Hidetoshi Kotera, Norio Nakatsuji, Yoshiki Sawa, Yong Chen, and Li Liu

1 Supplementary Materials for

2

3 **Human Pluripotent Stem Cell-Derived Cardiac Tissue-Like Constructs for Repairing of**
4 **the Infarcted Myocardium**

5

6 Junjun Li^{†a, b}, Itsunari Minami^{†a, c}, Motoko Shiozaki^c, Leqian Yu^{a, b}, Shin Yajima^c, Shigeru

7 Miyagawa^c, Yuji Shiba^d, Nobuhiro Morone^{a, §}, Satsuki Fukushima^c, Momoko Yoshioka^a, Sisi

8 Li^{a, e}, Jing Qiao^{a, b}, Xin Li^a, Lin Wang^a, Hidetoshi Kotera^b, Norio Nakatsuji^a, Yoshiki Sawa^{c*},

9 Yong Chen^{a, e*}, Li Liu^{a, b*}

10

11

12

13

14

15

16

17

18

19

20

21

22

23

24

25 **Supplemental experimental procedures**

26 **Nanofiber Fabrication**

27 Poly(D,L-lactic-co-glycolic acid) (PLGA, 75/25, Sigma, USA) was mixed with
28 tetrahydrofuran (THF, Wako, Japan) at different concentrations: 20%, 23%, and 25% (w/v);
29 then, ionic surfactant sodium dodecyl sulphate (SDS, Wako, Japan) dissolved in de-ionized
30 water was added to a final concentration of 0.92 g L⁻¹. For fluorescent labeling, PLGA
31 solution was loaded with fluorescein isothiocyanate (FITC) or Alexa Fluor® 594 (Life
32 Technologies, USA). PLGA nanofibers were fabricated by electrospinning at the voltage of
33 10 kV provided by a DC high-voltage generator (Tech Dempaz, Japan). The solution was
34 loaded into a 1-mL syringe to which a needle with a 0.6-mm inner diameter was attached; the
35 positive electrode of the high-voltage power supply was connected to the needle. A grounded
36 rotating drum was used at the speed of 11.4 m s⁻¹ to generate aligned nanofibers (ANFs);
37 random nanofibers (RNFs) were generated without rotation. The thickness of nanofibers was
38 controlled by varying the spin time: 10 min for high-density ANFs (H-ANFs, 11.3 ± 1.2 µm),
39 40 s for low-density ANFs (L-ANFs, 1.5 ± 0.1 µm) and 20 s for RNFs (1.5 ± 0.1 µm). The
40 distance between the tip and collector was maintained at 8 cm. Before spinning, a layer of
41 aluminium foil was attached to the drum for the fiber transfer procedure. Nanofibers were
42 collected in the aluminium foil which was then peeled off and pressed onto the substrate by a
43 thermal press machine (AS ONE, Japan) or transferred to a poly-dimethylsiloxane (PDMS)
44 frame (1 × 1 cm²); then, the foil was removed and nanofibers remained on the substrate or
45 PDMS frame.

46 **Electrophysiological Characterization**

47 Extracellular recording of field potentials (FPs) was performed using the multielectrode array
48 (MEA) data acquisition system (USB-ME64-System, Multi Channel Systems, Germany).

49 Signals were recorded from day 2 after CM seeding. The data were collected and processed
50 using MC_Rack (Multi Channel Systems) or LabChart (ADInstruments, New Zealand).

51 Electrical activation was started by applying bipolar stimuli (± 1500 mV, 40 μ s) in the
52 electrodes at the MEA centre. The local activation time (LAT) for a single electrode was
53 determined by calculating the minimum of the first derivative plot of the original data. The
54 isochronal map was constructed based on linear interpolation between the electrodes (Meiry
55 et al., 2001), calculated using the Matlab function (Matlab, MathWorks, America). The
56 amplitude, QT interval, and beating rate were determined by analyzing the wave form, and
57 the corrected cQT interval was calculated by normalization to the CM beating rate using the
58 Fridericia correction formula: $cQT \text{ interval} = QT \text{ interval} / \sqrt[3]{RR \text{ interval}}$. To assess the effects
59 of different drugs, E-4031, isoproterenol, propranolol, Verapamil and Quinidine were added
60 to 1 mL of medium respectively between 6-14 day after cell seeding.

61 **Electron Microscopy**

62 Top view high-resolution images were obtained using a scanning electron microscope (SEM
63 JCM-5000; JEOL Ltd., Japan) operating at 10 kV. CM samples were fixed with 4%
64 paraformaldehyde (PFA; Wako) for 2 min at room temperature, washed twice with PBS,
65 immersed in 30% ethanol for 30 min, and dehydrated in a series of ethanol concentrations
66 (50%, 70%, 80%, 90%, and 100%) for 10 min per each step, followed by nitrogen drying. A
67 5-nm-thick platinum layer was deposited on the samples by sputtering (MSP 30T; Shinku
68 Device, Japan).

69 For transmission electron microscopy (TEM), the samples were fixed with 2% glutaraldehyde
70 (Distilled EM Grade, Electron Microscopy Sciences, USA) in NaHCa buffer (100 mM NaCl,
71 30 mM HEPES, 2 mM $CaCl_2$, adjusted to pH 7.4 with NaOH) and successively post-fixed

72 with 0.25% OsO₄/0.25% K₄Fe(CN)₆, then with 1% tannic acid, and finally with 50 mM
73 uranyl acetate. The samples were washed, dehydrated in a series of ethanol, and embedded in
74 TABA EPON 812 resin (TAAB Laboratories Equipment Ltd, UK). After polymerization at
75 65°C, ultrathin sections (60–100 nm) were cut perpendicular to PLGA fibers using an
76 ultramicrotome (Leica FC6, Austria), mounted on EM grids, stained with lead citrate, and
77 analyzed by TEM (JEOL JEM1400, Japan).

78 **Histology**

79 Tissues were washed three times with PBS, fixed in 4% PFA in PBS, and embedded in
80 paraffin. Thin sections were cut, stained with hematoxylin and eosin (Muto chemical
81 corporation, Japan). Capillary density and inflammatory reactions were assessed by
82 immunohistolabeling for CD31 (mouse monoclonal IgG, 1:50; Dako: M0823) or CD68
83 (mouse monoclonal IgG, 1:100; Abcam: 955) respectively. The sections were observed under
84 a CKX41 microscope (Olympus) or a BIOREVO fluorescence microscope (KEYENCE
85 Corporation).

86 **Immunostaining and Imaging**

87 CMs were fixed in 4% PFA at room temperature for 30 min, permeabilized with 0.5% v/v
88 Triton X-100 in Dulbecco's (D)-PBS at room temperature for 1 h, and incubated in blocking
89 solution (5% v/v normal goat serum, 5% v/v normal donkey serum, 3% v/v bovine serum
90 albumin, and 0.1% v/v Tween 20 in D-PBS) at 4°C for 16 h. CMs were then incubated with
91 primary antibodies: anti-β-MHC (mouse monoclonal IgM, 1:100; Santa Cruz Biotechnology:
92 SC-53089), anti-α-actinin (mouse monoclonal IgG, 1:1000; Sigma: A7811), and anti-cTnT
93 (mouse monoclonal IgG, 1:200; Santa Cruz Biotechnology: SC-20025) at 4°C for 16 h. Cells
94 were washed and incubated with appropriate secondary antibodies diluted 1:300 in blocking

95 buffer: DyLight-594 anti-mouse IgM (Jackson ImmnoResearch: 715-516-020), Alexa Fluor
96 594 anti-rabbit IgG (Jackson ImmnoResearch: 711-586-152), Alexa Fluor 594 anti-mouse
97 IgG (Jackson ImmnoResearch: 715-586-150), and Alexa Fluor 488 anti-rabbit IgG (Jackson
98 ImmnoResearch: 711-546-152) at room temperature for 1 h. Cell were counterstained with
99 300 nM 4'-6-diamidino-2-phenylindole (DAPI, Wako) at room temperature for 30 min to
100 visualize the nuclei. Images were captured using a fluorescent or confocal microscopes
101 (Olympus), and the orientation of CMs and nanofibers was evaluated by the Fourier
102 component analysis using the ImageJ Directionality plugin (Woolley et al., 2011) which
103 assessed the orientation distribution for each color channel. Tomography images were
104 acquired and combined to form 3D images using the Optical Coherence Microscopy system
105 and the white-light Linnik interferometer (OCM system, Panasonic).

106 For immunostaining after transplantation, tissues were rinsed with PBS, cut, immersed in
107 30% sucrose in PBS, and embedded in O.C.T. compound (Sakura Finetek USA, Inc.). Frozen
108 sections were cut into 7- μ m-thick slices using a cryostat (Leica CM 1950) and mounted on
109 MAS-coated glass slides (Matsunami Glass Ind. Ltd.). After treatment with PBS or Tris-
110 buffered saline (TBS) containing 1% bovine serum albumin (BSA) and 0.05% Tween 20, the
111 sections were incubated with a mouse anti-cardiac troponin T antibody (2–10 μ g/mL; Abcam
112 Plc: ab8295), a rabbit anti-cardiac troponin I (rabbit monoclonal IgG, 1:100; Abcam Plc:
113 ab52862) or a mouse anti-human nuclear antibody (HNA) (mouse monoclonal IgG, 1:200;
114 MED Millipore: MAB1281) for 16 h at 4°C, followed by incubation with secondary anti-
115 mouse Alexa 555-conjugated IgG (1:200; Life Technologies: A21422), anti-rabbit Alexa 555-
116 conjugated IgG (1:200; Life Technologies: A21428), anti-mouse Alexa 488-conjugated
117 IgG (1:200; Life Technologies: A11001) and anti-rabbit Alexa 488-conjugated
118 IgG (1:200; Life Technologies: A11008). F-actin was stained using Alexa Fluor 647-labelled
119 phalloidin (1:100; Life Technologies: A22287). The sections were mounted with the

120 ProLong Gold antifade reagent with DAPI (Life Technologies) and examined under a
121 confocal laser scanning microscope (FV1200; Olympus Co.) at the excitation wavelengths of
122 405, 488, 543, and 635 nm.

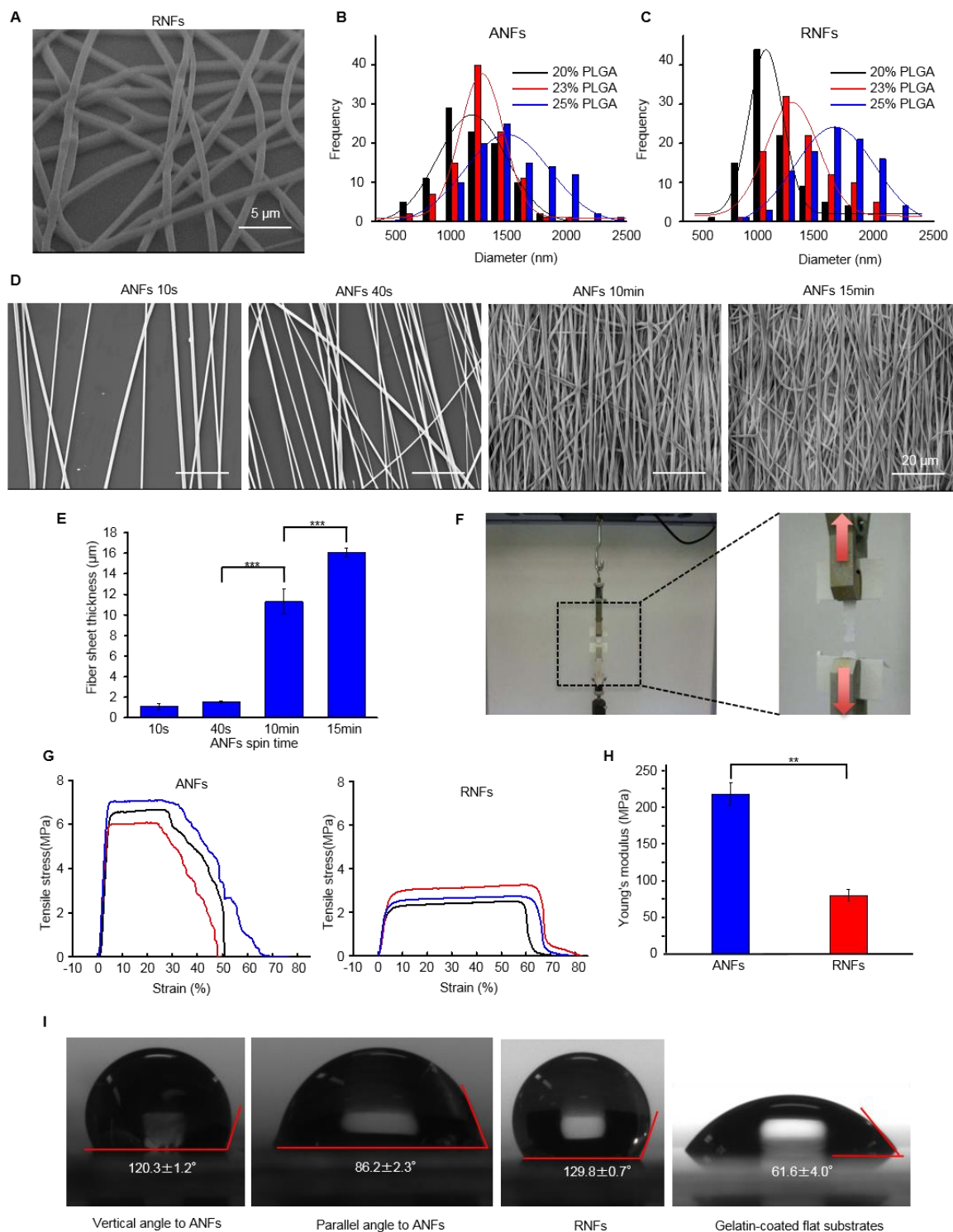
123 **Flow Cytometry**

124 HiPSCs-CMs cultured on different substrates were harvested using TrypLE Express solution
125 (Life Technologies), fixed in 4% PFA at room temperature for 30 min, permeabilized with
126 0.5% v/v Triton X-100 in Dulbecco's (D)-PBS at room temperature for 30 min, incubated
127 with anti-cTnT antibodies (mouse monoclonal IgG, 1:200; Santa Cruz Biotechnology: SC-
128 20025) or isotype-matched antibodies (BD Phosphoflow: 557782) at 37 °C for 30 min,
129 washed with D-PBS, and incubated with Alexa Fluor 488 anti-mouse IgG (1:500; Jackson
130 ImmnoResearch: 715-546-150). Cells were then washed twice with D-PBS and analyzed
131 using a FACS Canto II flow cytometer (BD Biosciences, USA) and the FlowJo software
132 (Treestar Inc., USA). Data shown are representative of at least
133 three independent experiments.

134 **qPCR**

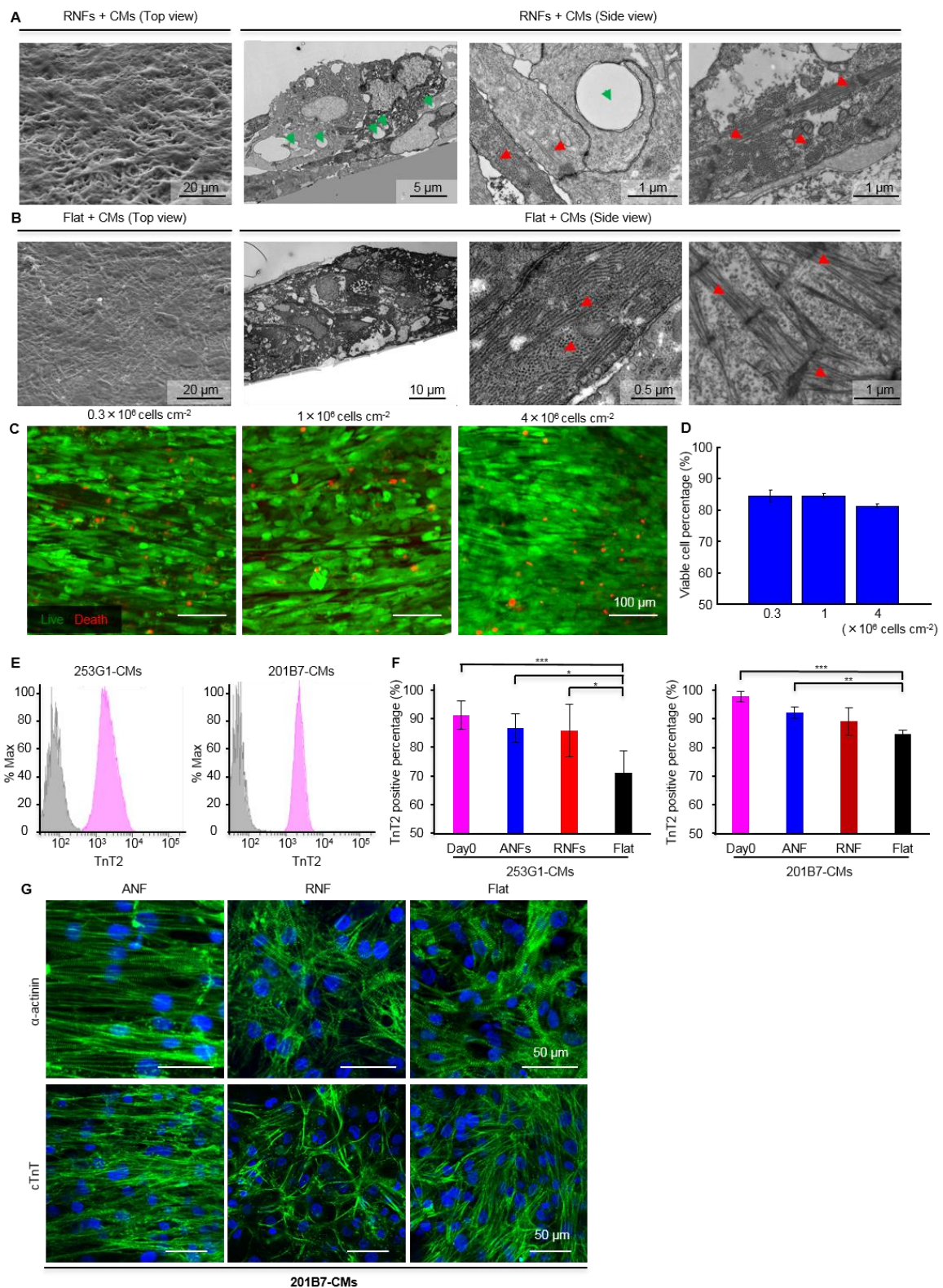
135 Total RNA was harvested using Trizol (Life Technologies), and RNA concentration was
136 measured using a NanoDrop1000 spectrophotometer (Thermo Fisher Scientific, USA). cDNA
137 was synthesized and analyzed by qPCR using the SYBR Green PCR MasterMix (Life
138 Technologies) and the qBiomarker Validation PCR Array (IPHS-102A; Qiagen, USA) in a
139 96-well format following the manufacturer's instructions. The cycling conditions were as
140 follows: initial denaturation at 95°C for 10 min, followed by 40 cycles at 95°C for 15 s and
141 60°C for 1 min; the reactions were performed in a StepOnePlus Real-Time PCR system (Life
142 Technologies). The gene expressions were measured by ddCt method relative to house keep

143 gene (GAPDH). Heatmaps were generated by the R package open-source software for
 144 bioinformatics. The clustering order was produced with Ward.D clustering algorithm.



145
 146 **Figure S1. Characteristics of nanofibers. Related to Figure 1.** (A) A representative
 147 electron microscopy image of randomly arranged nanofibers (RNFs). (B, C) Diameter
 148 distribution of aligned nanofibers (ANFs, B) and RNFs (C) fabricated with different
 149 concentrations of poly(D,L-lactic-co-glycolic acid) (PLGA). (D) Electron microscopy images

150 of ANFs manufactured using different spin times (10 s, 40 s, 10 min, and 15 min). **(E)** ANFs
151 thickness depending on the spin time. Data are represented as means \pm SD, n = 4 independent
152 experiments. ***p < 0.001 by One-way ANOVA followed by Tukey's post hoc test. **(F)**
153 Photographs of the experimental setup. Specimen gauge length and width were determined
154 using a Shimadzu Autograph AGS-X micro-tensile tester (Shimadzu Corp.) with a 1N load
155 cell and digital video extensometer, setting the cross-head speed at 10 mm min⁻¹. The rigidity
156 was calculated using Trapezium X with an initial linear region of the stress-strain curve. **(G)**
157 Stress-strain curves of aligned nanofibers (ANFs) and random nanofibers (RNFs). **(H)**
158 Young's modulus of ANFs and RNFs. Data are represented as means \pm SD, n = 3 independent
159 experiments. **p < 0.01 by Student's t test. **(I)** Contact angle measurement of ANF/RNF and
160 gelatin-coated flat substrates. The sessile drop method was used to measure the contact angle
161 of a water droplet on the substrate using a microscope with a CCD camera. A 2- μ L water
162 droplet was deposited onto the substrate and the water/substrate interface was photographed.
163 The edge of the droplet was then analyzed using a sessile drop-fitting model. Data are
164 represented as means \pm SD, n = 3 independent experiments.

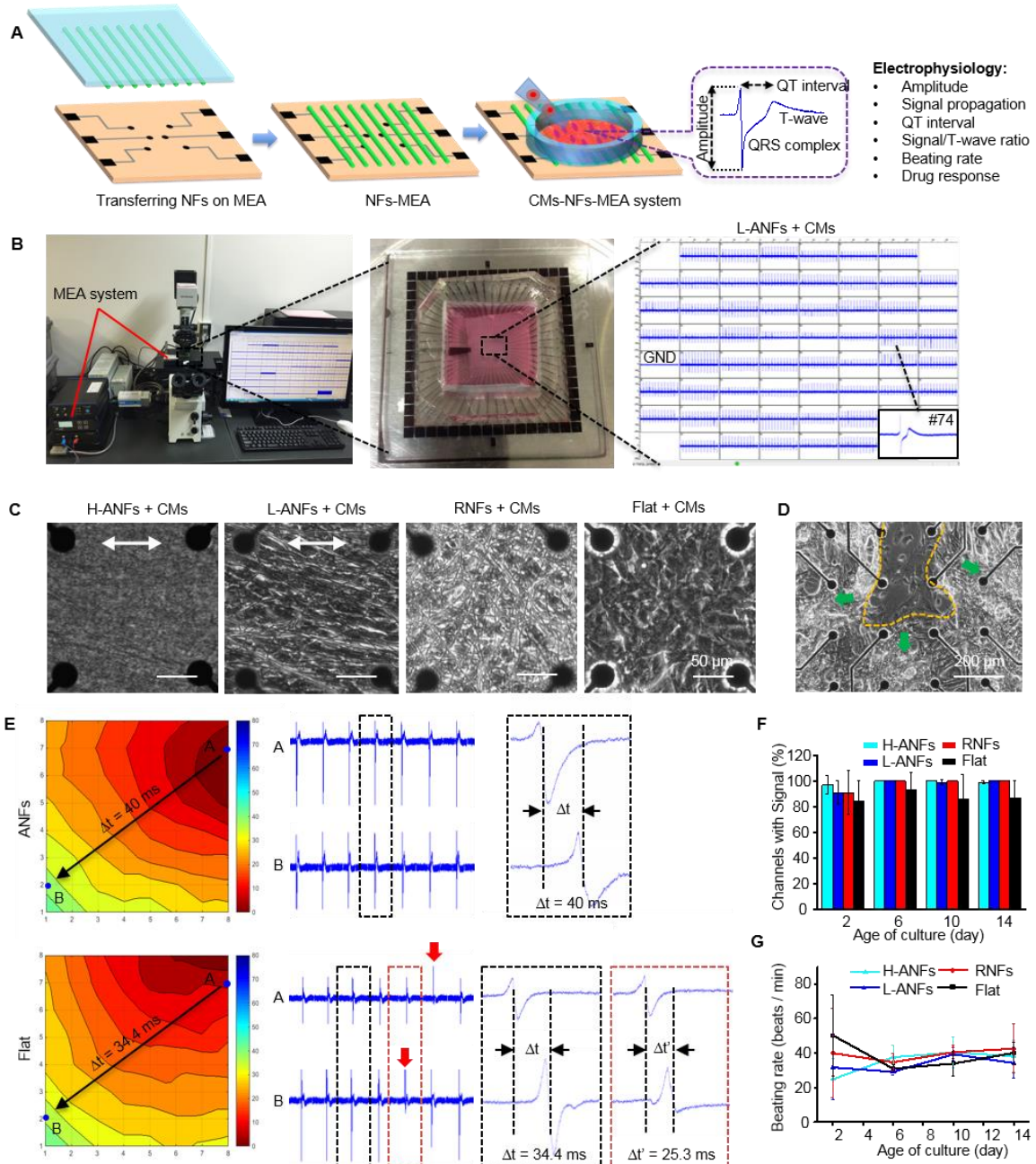


165
166

167 **Figure S2. Tissue formed on different substrates. Related to Figure 1 and Figure 2. (A)**
 168 Scanning electron microscopy (SEM, top view) and transmission electron microscopy (TEM,
 169 side view) images of cardiomyocytes (CMs) cultured on random nanofibers (RNFs) for 14
 170 days. **(B)** SEM (top view) and TEM (side view) images of CMs cultured on Flat for 14 days.
 171 The green and red arrows indicate nanofibers and sarcomeric bundles in the actin-myosin
 172 system, respectively. **(C, D)** Viability of CTLCs with different cell densities on day 6. Data

173 are represented as means \pm SD, n = 3 independent experiments. **(E)** Flow cytometry data of
174 cTnT positive cell (hiPS cell line: 253G1; 201B7) on day 0. **(F)** Flow cytometry analysis of
175 CMs on different substrates: aligned nanofibers (ANFs), random nanofibers (RNFs), and
176 gelatin-coated flat substrate (Flat) for 14 days. Data are represented as means \pm SD. For
177 253G1, Day 0: n = 32; ANFs: n = 3; RNFs: n = 3; Flat: n = 3; For 201B7, n = 3 (n represents
178 independent experiments for all the groups). *p<0.05, **p<0.01 and ***p < 0.001 by One-
179 way ANOVA followed by Tukey's post hoc test. **(G)** Immunostaining images of α -actinin and
180 cTnT (green). Cardiomyocytes (CMs, 201B7) were cultured on different substrates for 14
181 days.

182

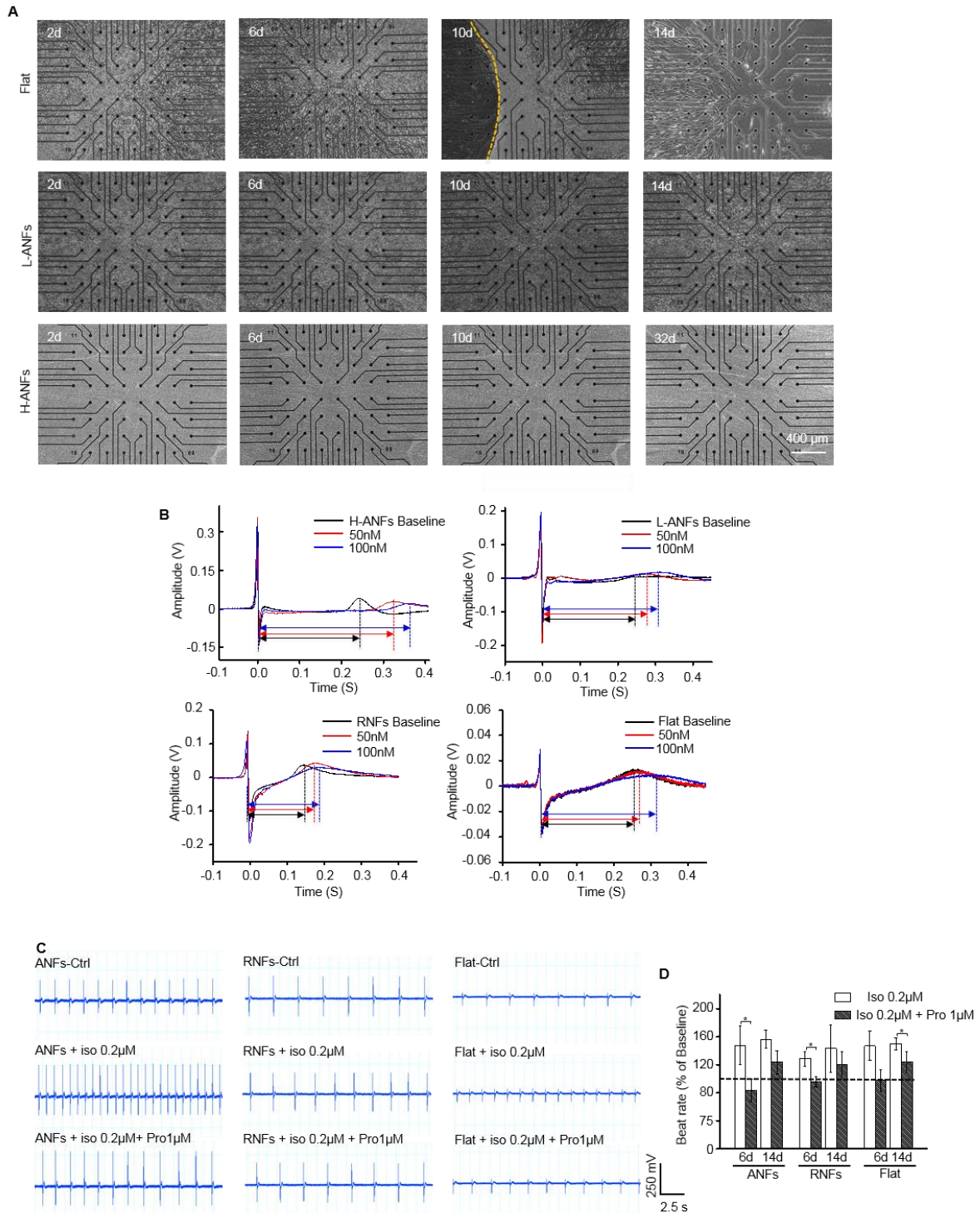


184

185 **Figure S3. Extracellular recording of cardiomyocytes (CMs) using the microelectrode**
 186 **array (MEA). Related to Figure 3. (A)** Schematic representation of cardiac tissue-like
 187 construct (CTLC) integration into the MEA system. The encircled image is a representative
 188 electrogram of the field potential (FP) recorded from CMs, illustrating the parameters to be
 189 analyzed. **(B)** Images of the MEA system and MEA chip with CTLC. The enlarged images
 190 indicate the homogeneous electrical signals recorded by electrodes. **(C)** Phase contrast
 191 images of CMs on different substrates: high-density and low-density aligned nanofibers (H-
 192 ANFs and L-ANFs, respectively), random nanofibers (RNFs), and gelatin-coated flat
 193 substrates (Flat). The white arrows mark ANFs orientation. **(D)** Images of the Flat sample on
 194 day 6 with CMs clusters marked by green arrows. The dashed line marks the area with few
 195 remaining CMs. **(E)** Homogeneity and regularity of CM beating on ANFs and Flat.
 196 Activation maps (left) illustrate homogeneous propagation of spontaneous contractions;
 197 contraction regularity is shown by a series of beatings (right) recorded from point A to B,
 198 with a delay of Δt . The red arrows mark irregular beating which resulted in different $\Delta t = 25.3$

199 ms. **(F)** Channels recording field potential ($n = 6-8$ independent biological replicates). **(G)**
 200 CM beating rate at different culture times ($n = 3-5$ independent biological replicates). Data
 201 are represented as means \pm SD.

202

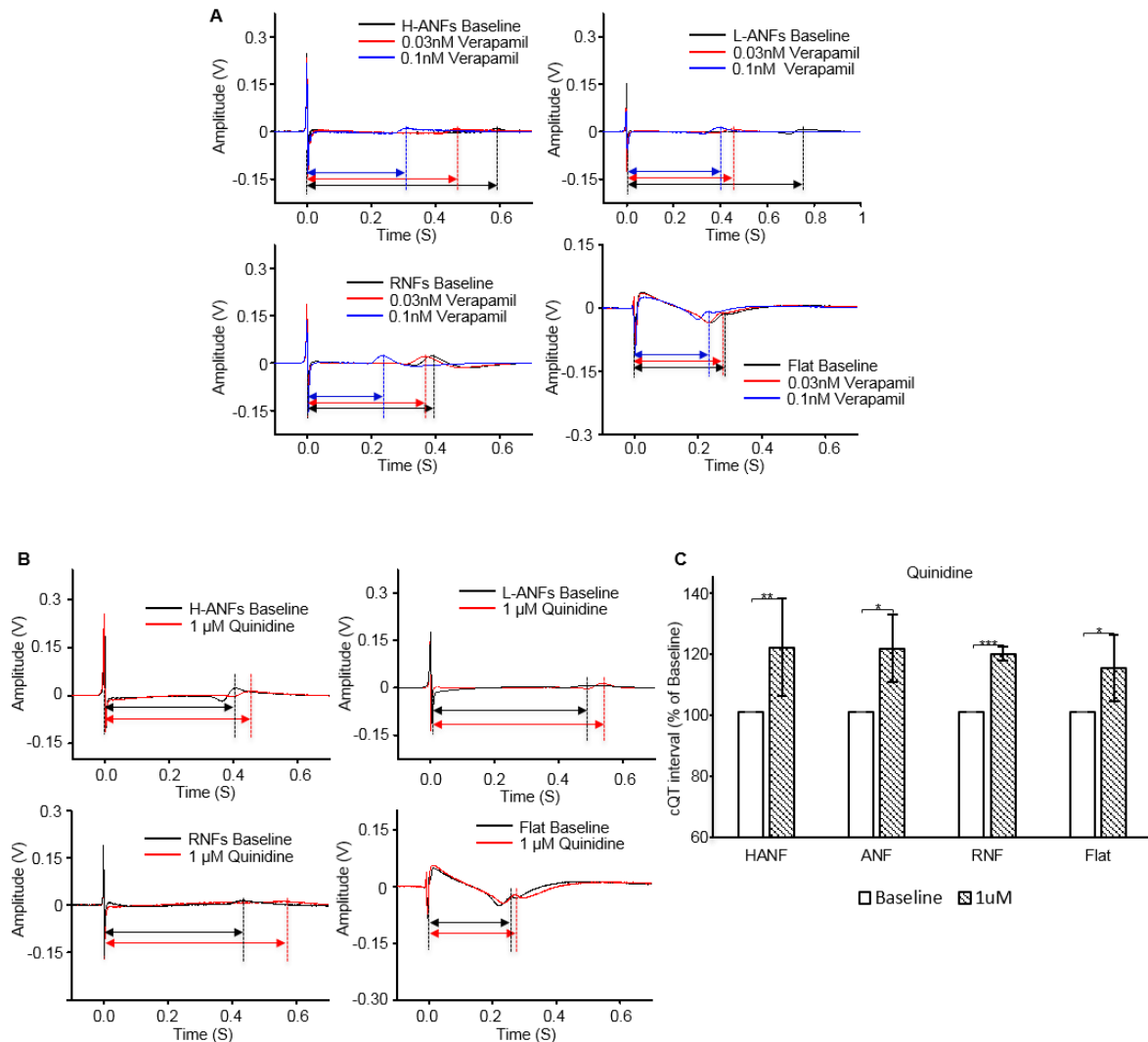


203

204 **Figure S4. Long term culture and drug effects on cardiomyocytes (CMs). Related to**
 205 **Figure 3. (A)** Long-term culture of cardiomyocytes (CMs) on gelatin-coated flat substrates
 206 (Flat) and low-density and high-density aligned nanofibers (L-ANFs and H-ANFs,
 207 respectively). The dashed line marks the area where the CM sheet peeled off from the

208 substrates; the CM sheet totally peeled off from Flat on day 14. Cardiac tissue-like constructs
 209 (CTLCs) created on H-ANFs were sustained for over 32 days. **(B)** Prolongation of the
 210 repolarization phase after E4031 application. **(C)** Representative beating of CMs treated with
 211 isoproterenol (Iso) and propranolol (Pro) and cultured on different substrates. **(D)** Effects of
 212 Iso and Pro on CM beating rate. Data are represented as means \pm SD, $n = 3-4$ independent
 213 biological replicates. * $p < 0.05$ by Student's t test.

214



215

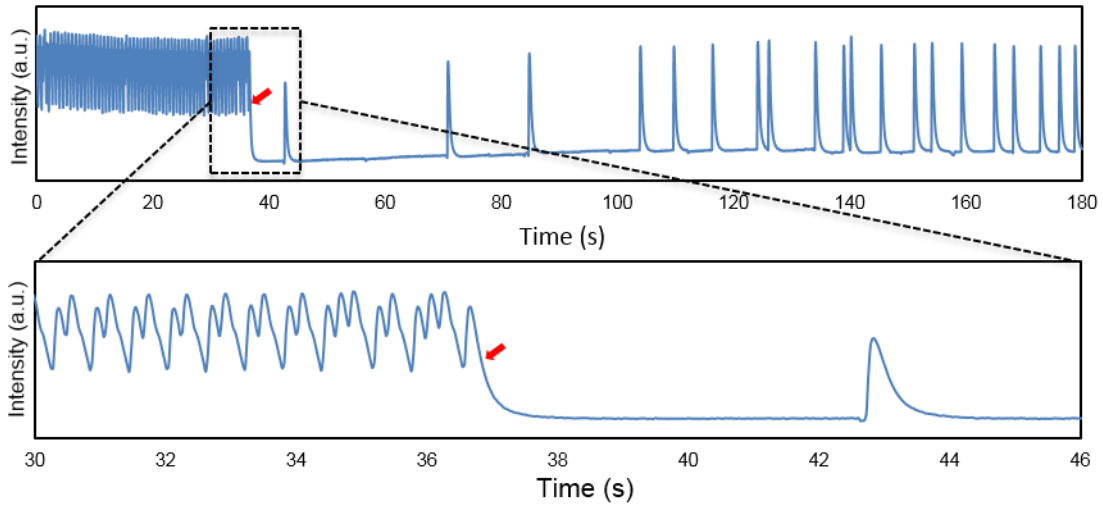
216 **Figure S5. Drug effects on cardiomyocytes (CMs). Related to Figure 3. (A)** Shortening of
 217 the repolarization phase after verapamil application. **(B)** Prolongation of the repolarization
 218 phase after quinidine application. **(C)** Effects of quinidine on corrected QT interval (cQT
 219 interval) of CM beating. Data are represented as means \pm SD, $n = 3-7$ independent biological
 220 replicates. * $p < 0.05$, ** $p < 0.01$, and *** $p < 0.001$ by Student's t test.

221

222

223

224

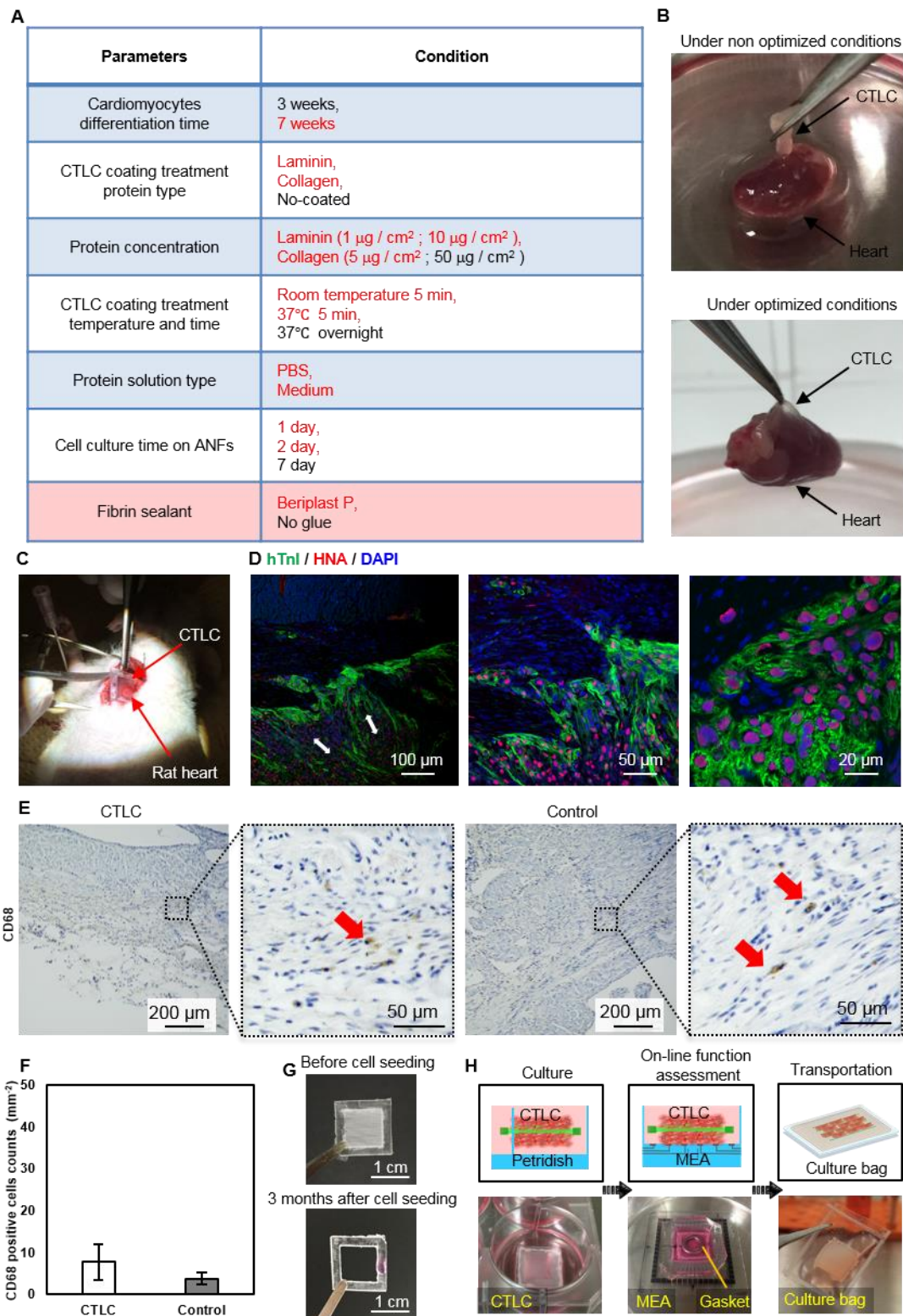


225

226 **Figure S6 Ca^{2+} transients of the GCaMP3-positive CTLC on a host CM sheet with**
227 **spiral waves. Related to Figure 4.** The recording lasted for 3 min and the red arrow marked
228 the moment when the spiral wave was terminated by the coupling of CTLC with the host CM
229 sheet.

230

231



232

233 **Figure S7. Preparation of a cardiac tissue-like construct (CTLC) for transplantation.**
 234 **Related to Figure 5 and Figure 6. (A)** Condition screening by the *in vitro* attachment to
 235 mouse hearts. To improve CTLC attachment to the heart, a number of experimental
 236 conditions were screened. The conditions marked in red were used for transplantation. **(B)**
 237 CTLC attachment was assessed *in vitro* by testing whether the mouse heart-bound CTLC
 238 could sustain the weight of the heart. **(C)** Transplantation of CTLC on a rat heart. **(D)** Double
 239 immunostaining of consecutive sections from the *in vivo* transplanted CTLC for human

240 cardiac troponin I (hTnI) and human nuclear antigen (HNA); nuclei were stained with DAPI.
241 The white arrow indicated the alignment of CMs. **(E)** Long-term degradation of nanofibers.
242 Aligned nanofibers (ANFs) were mounted onto a PDMS frame (top) and immersed in
243 medium after seeding of cardiomyocytes (CMs); ANFs would degrade within 3 month
244 (bottom). **(E)** Immunohistochemical analysis on peri-ischemic zone in MI heart 4 week after
245 transplantation of CTLC (left) and acellular control (right). The sections are immunostained
246 with CD68 antibodies. The red arrow marked the CD68-positive cells. **(F)** The CD68 positive
247 cells density in CTLC and control group. Data are represented as means \pm SD, n = 3 rats. **(G)**
248 Preparation and transport of the CTLC. After cell seeding, the CTLC can be functionally
249 evaluated before transportation and used for other applications. A gasket is used to fix the
250 CTLC on the MEA for signal recording.

251

252 **REFERENCES**

253

254 Meiry, G., Reisner, Y., Feld, Y., Goldberg, S., Rosen, M., Ziv, N., Binah, O. (2001). Evolution of
255 action potential propagation and repolarization in cultured neonatal rat ventricular
256 myocytes. *J. Cardiovasc. Electrophysiol.* *12*, 1269-1277.

257 Woolley, A.J., Desai, H.A., Steckbeck, M.A., Patel, N.K., Otto, K.J. (2011). In situ
258 characterization of the brain-microdevice interface using device-capture histology. *J.*
259 *Neurosci. Methods* *201*, 67-77.

260